L3 Note 2455
September 1, 1999

TWO PHOTON PHYSICS AT LEP

MANEESH WADHWA
University of Basel, Klingelbergstrasse 82,
CH-4056 Basel, Switzerland
E-mail:Maneesh.Wadhwa@cern.ch

LEP offers an excellent opportunity to measure two photon processes over a large kinematical range and thus study the complex nature of the photon. This article reviews the experimental status of "Two Photon Physics" at LEP. The recent results on resonances, multi-hadron production and photon structure functions are discussed.

1 Introduction

Over the past decade two photon physics has proven to be a very productive source of information about QED, QCD and hadron spectroscopy. The Feynman diagram responsible for a two photon collision process at LEP is shown in Figure 1, where the high energy incident electrons and positrons split off virtual photons and the scattered electrons take most of the beam energy. These two photons then can interact to form a state X with mass $W_{\gamma\gamma}$. The four-momentum transfer q_i to the photons depends on the angle and energy of the scattered electrons[a]. When neither of the scattered electrons is detected (untagged events), the virtual photons are referred to as nearly real i.e. $q_1^2 \approx q_2^2 \approx 0$. This class of events allows several tests of QCD by studying hadronic resonances, the inclusive hadron cross section and jet production rates. If there is detection of one of the scattered electrons $Q^2 = -q_1^2$ (single tagged events), it is possible to probe the other photon $q_2^2 \approx 0$ regarded as a "target" and study its structure. Finally, if both the

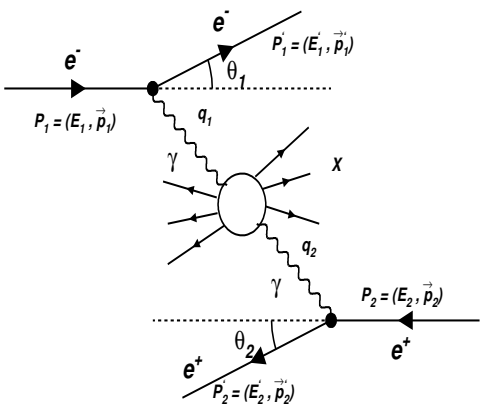

Figure 1. *$\gamma\gamma$ collision in* e^+e^- *scattering*

[a]Electron stands for electron and positron throughout this article

scattered electrons are detected $Q_i^2 = -q_i^2, (i = 1, 2)$ (double tagged events), the structure of the reaction of highly virtual photons is probed. In the following sections, a review is given of the $\gamma\gamma$ results obtained at LEP, with special attention to recent results.

2 Resonance production

Two photon formation of C-even meson resonances provides valuable information on the internal structure of mesons. In particular it is interesting to look for resonances whose $\gamma\gamma$ couplings are much smaller than quark-model predictions; e.g. glueball or hybrid quark-gluon states. One can also produce resonances in two-photon events in which one photon is far off mass shell. The interest in this case is twofold. First, the meson transition form factor can be measured and secondly spin-1 states can be produced.

Table 1. *List of resonances studied at LEP*

Resonance	Final state	J^{PC}	$\Gamma_{\gamma\gamma}$(keV)
$\eta^{'}$ (958)	$\pi^+\pi^-\gamma$	0^{-+}	$4.17 \pm 0.10 \pm 0.27$ [1]
a_2 (1320)	$\pi^+\pi^-\pi^0$	2^{++}	$0.98 \pm 0.05 \pm 0.09$ [2]
$a_2^{'}$ (1750)	$\pi^+\pi^-\pi^0$	2^{++}	$0.29 \pm 0.04 \pm 0.02/(\mathrm{BR})$ [2]
$f_2^{'}$ (1525)	$K_s^0K_s^0$	2^{++}	$0.09 \pm 0.02 \pm 0.02/(\mathrm{BR})$ [3]
η (1440)	$K_s^0K\pi$	0^{-+}	$0.17 \pm 0.05/(\mathrm{BR})$ [4]
η_c (2980)	12 Channels	0^{-+}	$8.0 \ \pm 2.3 \ \pm 2.4$ [5]
η_c (2980)	9 Channels	0^{-+}	$6.9 \ \pm 1.9 \ \pm 2.0$ [6]
$\chi_{c2}(3555)$	$J/\psi\ \gamma$	2^{++}	$0.97 \pm 0.40 \pm 0.36$ [7]

At LEP, many exclusive channels are studied as shown in Table 1. Two recent results are discussed in the following sections.

2.1 Charmonium Production

Measurements of the charmonium system in the two photon collisions are mainly motivated by the large quark mass, where the predictions are reliable, which provides a test of perturbative QCD. Using LEP I and LEP II data, with a total luminosity of 193 pb^{-1} , the charmonium resonance η_c is observed[6] and reconstructed in nine different decay modes. The two photon partial width of the η_c is extracted to be $\Gamma_{\gamma\gamma} = 6.9 \pm 1.9 \pm 2.0$ keV. Figure 2 (a) shows the invariant mass distribution of selected events with one of the scattered electron tagged in the forward calorimeter. The spectrum is fitted with a

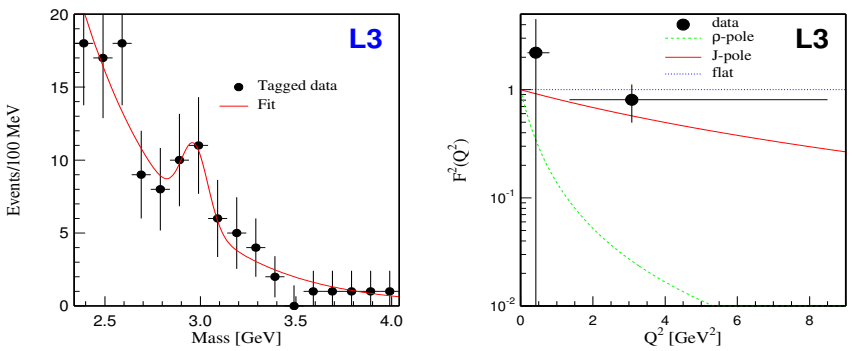

(a) (b)

Figure 2. *(a) The η_c invariant mass spectrum , (b) the η_c form factor, fitted with a VDM pole form, with pole mass equal to* $M_{J/\psi}$.

Gaussian for the signal and a exponential for the background. These events allow to measure the η_c transition form factor in different Q^2 bins, (0.2 GeV^2 $< Q^2 <$ 9 GeV^2). Figure 2(b) shows the η_c form-factor measurement by L3, which favors the form-factor with a J/ψ mass pole in the VDM model and are in agreement with theoretical calculations[10].

2.2 $K^0_s K^0_s$ Resonances and GlueBall Search

The resonance formation process $\gamma\gamma \rightarrow R \rightarrow \mathrm{K}^0_s\mathrm{K}^0_s \rightarrow \pi^+\pi^-\pi^+\pi^-$ has been studied[3] with the L3 detector. The $\mathrm{K}^0_s\mathrm{K}^0_s$ mass spectrum Figure. 3, shows clear evidence for the formation of the $f_2^{'}(1525)$ tensor meson. Around 1300 MeV, $f_2(1270) - a_2(1320)$ destructive interference is observed consistent with theoretical predictions[11]. In addition, there is an enhancement of ≈6 standard deviations around 1750 MeV which is possibly due to the formation of a radially excited state of the $f_2^{'}$, according

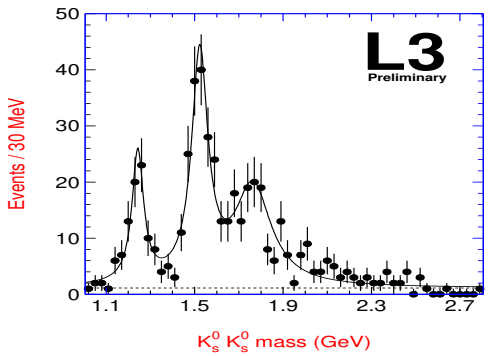

Figure 3. *The $K^0_s K^0_s$ mass spectrum*

to theoretical predictions[9]. The measured two photon partial width of the $f_2'(1525)$ is shown in Table 1. A study of the angular distribution of the f_2' in the two-photon centre-of-mass system favours helicity-2 formation over helicity-0, consistent with theoretical predictions[14].
A search for the glueball candidate ξ (2230) has been performed at LEP in the $K^0_s K^0_s$ decay channel. The search is motivated due to the previous observation of ξ (2230) by the Mark III Collaboration[13] which has been confirmed by BES Collaboration[12]. At LEP, non observation of signal gives an upper limit for $\Gamma_{\gamma\gamma}(\xi(2230)) \times \mathrm{Br}(\xi(2230) \to K^0_s K^0_s) < 1.5$ eV at 95% CL under the hypothesis it is a pure spin 2, helicity two state. This low value is most likely inconsistent with a $q\bar{q}$ assignment to the $\xi(2230)$.

3 The Two Photon Total Cross-section

At LEP II energies, the two photon process $e^+e^- \to e^+e^-\gamma^*\gamma^* \to e^+e^-hadrons$ is a copious source of hadron production. In this reaction the photons either interact as a point-like particle or undergo quantum fluctuation (resolved photon) into a resonant(VMD) or non-resonant virtual states opening up all the possibilities of hadronic interactions as shown in Figure 4. These interactions can be described in terms of Regge poles[15,16], (Pomeron or Reggeon exchange).

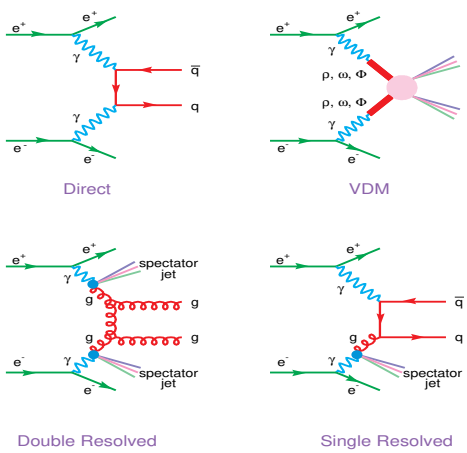

Figure 4. *Some diagram contributing to hadron production in $\gamma\gamma$ collisions at LEP.*

A measurement of the total hadronic cross section as a function of $\sqrt{s}$, improves our understanding of the hadronic nature of the photon. At LEP, using the high energy runs above the Z peak, L3 and OPAL have measured the cross section[17,18] $\sigma(\gamma\gamma \to hadrons)$ in the range $5 \leq W_{\gamma\gamma} \leq 145$ GeV as shown in the Figure 5.

The cross-section measurement of the two experiments show a clear rise at high energies, described by a "Soft Pomeron" and the data of the L3 experiment show a fast decrease at low energies due to "Reggeon exchange". The rise of $\sigma_{\gamma\gamma}$ is faster than the one observed in hadron-hadron or γp collisions; a simple factorization ansatz[19] $\sigma_{\gamma\gamma} = \sigma^2_{\gamma p}/\sigma_{pp}$ is excluded as can be seen in Figure 5 from the predictions of Schuler and Sjostrand[22]. The data are rather well described by the dual parton model of Engel and Ranft[23] or by analytical calculations which take into account the importance of QCD effects at high transverse momentum. In Figure 5, the minijet model of Godbole and Pancheri[24] is also represented. One has to notice that all models has some dependence which can change the cross section predictions by 10-30%. The Monte Carlo models PYTHIA and PHOJET which are used to correct the data, differ by ≈20% in the absolute normalization. In future, improvements in the theoretical predictions especially the description of diffractive processes are desirable.

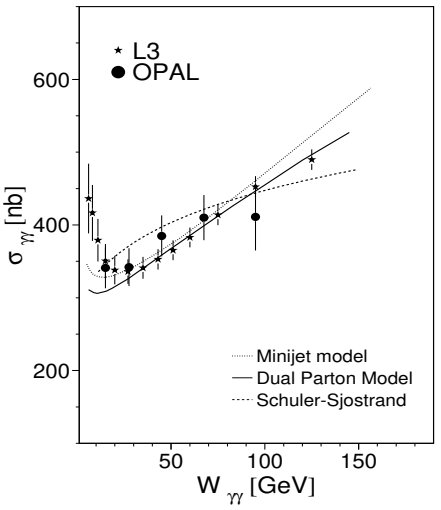

Figure 5. *The measured cross-section* $\sigma(\gamma\gamma \to hadrons)$ *as a function of* $W_{\gamma\gamma}$.

4 Single Particle and Jet Production

Inclusive production of charged hadrons, K^0_s mesons, and jet studies has been performed at LEP by the OPAL experiment. Figure 6(a) shows a measurement of differential cross-section for charged hadrons produced in collision of the two quasi-real photons in the range 10 GeV$<$ $W_{\gamma\gamma}$ $<$125 GeV as a function of transverse momentum[25] p_T . The

results are compared to NLO perturbative QCD calculations[26]. For lower values of $W_{\gamma\gamma}$, more charged hadrons than predicted are found at

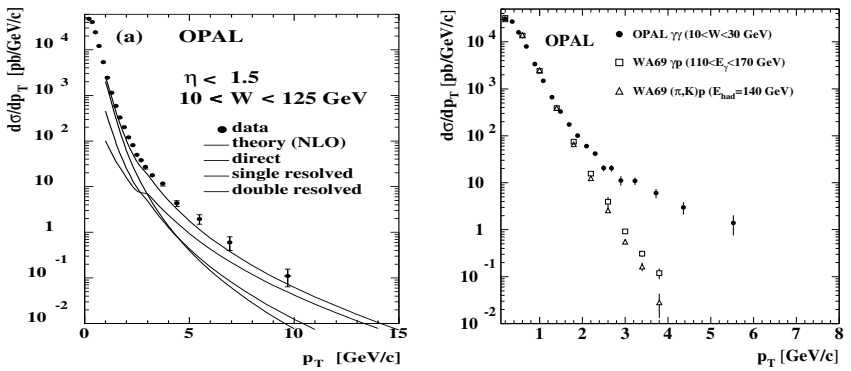

Figure 6. *a) Differential inclusive charged hadron cross-section and b) the* $\mathrm{p_T}$ *distribution measured in* $\gamma\gamma$ *interactions compared to the* γp *and* $(\pi,K)p$ *interactions.*

large p_T. Also shown in figure 6(b) is the comparison of the $\gamma\gamma$ data data to $\mathrm{p_T}$ measured in γp and (π, K)p interactions normalised at the same value at low p_T, one observes there is a significant increase of rates in the $\gamma\gamma$ process above a p_T of 2 GeV. The clear deviation from the hadronic interactions shows the effect of the direct component in the $\gamma\gamma$ interactions. Similar studies of p_T distributions of the K^0_s mesons are in reasonable agreement with NLO calculations[25].

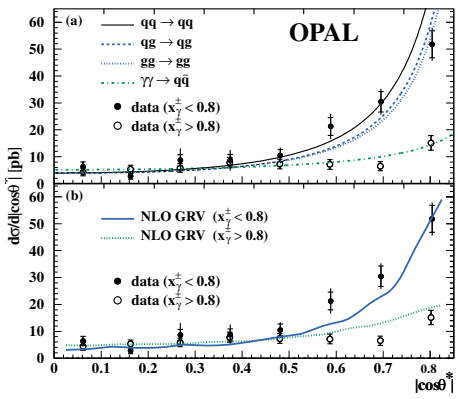

Figure 7. *The angular distribution in the dijet center-of-mass system for "Direct" and "Resolved" events*

The OPAL experiment has performed a very nice measurement of dijet production in two-photon collisions at $\sqrt{s}$ = 161 and 172 GeV. Their results[28] demonstrate that it is possible to distinguish between direct and resolved processes in the dijet events. With the help of the variable x_γ, which is the estimator of the fraction of the target pho-

ton's momentum carried by the parton which produces jets. Figure 7 shows the measured distribution of the parton scattering angle θ^* for direct and double-resolved processes, compared to the relevant QCD matrix element calculations[29]. One observes a clear distinction between the direct process $\gamma\gamma \to q\bar{q}$ ($x_\gamma > 0.8$), where a quark is exchanged in the t channel and the doubly resolved one ($x_\gamma < 0.8$), dominated by the gluon exchange. The strong rise in $\cos\theta^*$ distribution near $\cos\theta^*$=1 is due to a large double-resolved contribution, as expected from QCD.

5 Heavy Quark Production

The study of heavy quark (c,b) production in two photon collisions at LEP provides not only an excellent test of perturbative QCD but also gives an estimate of the gluon density in the photon. At LEP energies, the direct and resolved photon processes are predicted to give comparable contributions to the charm and beauty quark production cross-sections[30]. The resolved process is dominantly quark-gluon fusion: $\gamma g \to q\bar{q}$. The cross-section of the processes $e^+e^- \to e^+e^- c\bar{c}, b\bar{b}$ X has been measured by the L3[31] and OPAL[32] experiments. At L3, the charm and beauty quark are identified by tagging leptons (e, μ) from semileptonic charm and beauty decays. Charm quark were also identified by the reconstruction of $D^{\pm *}$ meson decays, where $D^* \to D^0\pi^\pm$, and OPAL tags charm quark with $D^* \to D^0\pi^\pm$ and $D^0 \to K^-\pi^+, K^-\pi^+\pi^o, K^-\pi^+\pi^-$.

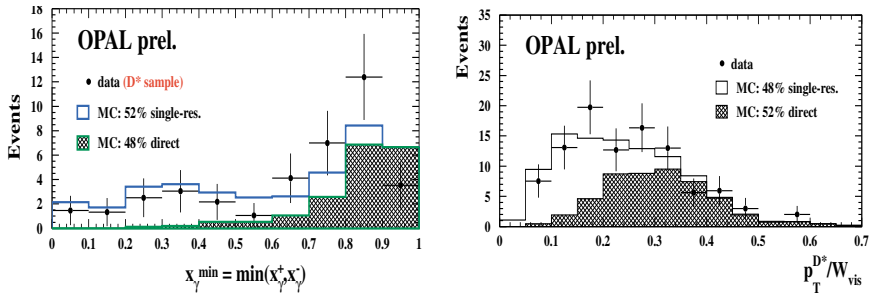

Figure 8. *The x_γ distribution of dijet events containing a D^* and the p_T distribution of the D^* normalised to the visible mass of the event.*

A good separation of direct and resolved processes is obtained by associating the D^* to a dijet analysis or by inspection of the p_T distribution of the D^* (See figure 8). As predicted the direct and resolved processes contribute roughly equally to the observed distribution. The differential D^* cross section

agrees well with the NLO predictions and is independent of the Monte Carlo models used to correct the data over the range of detector acceptance. The total inclusive cross-sections are plotted in Figure 9 together with previous measurements. The data are compared to NLO QCD calculations[30]. The direct process $\gamma\gamma \to c\bar{c}, b\bar{b}$, shown with dotted line, is insufficient to describe the data, even if real and virtual gluon corrections are included. The cross sections requires contributions from the resolved processes which are dominantly $\gamma g \to c\bar{c}, b\bar{b}$. The data therefore requires a significant gluon content in the photon.

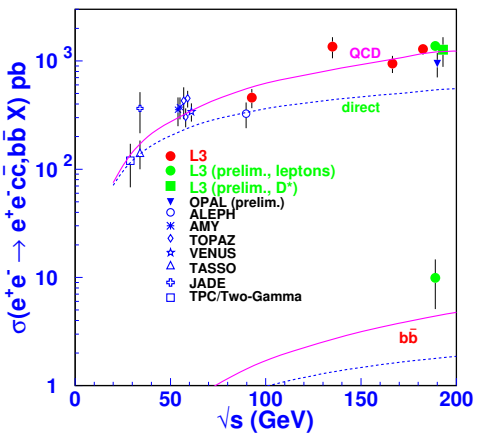

Figure 9. *The cross-section for heavy quarks production as measured at LEP and at previous* e^+e^- *colliders*

The $b\bar{b}$ cross section is measured for the first time in two photon collisions by the L3 experiment. The preliminary value of b cross section lie somewhat above QCD predictions.

6 Leptonic Structure Function, $F_2^{\gamma,QED}$

The leptonic structure function has been measured by all LEP experiments[33,34,35,36]. The measurement provides not only a QED test but also an experimental check for the procedures used in the study of the hadronic photon structure functions.

A result from L3, is shown as an example in figure 10 (a). It shows that it is possible to measure the effect of non-zero target photon virtuality. The analysis is performed using the $e^+e^- \to \mu^+\mu^-$ sample, for a range of Q^2 ($1.4 < Q^2 < 7.6$ GeV^2). The fit to $F_2^{\gamma,QED}$ corresponds to a target photon virtuality of 0.33 ± 0.005 GeV^2, in good agreement with QED predictions, if initial state radiative corrections are included.

Also shown in Figure 10 (c), is the measurement of the F_A and F_B structure functions , obtained by studying the azimuthal angle distribution of the μ^- in the $\gamma\gamma$ centre-of-mass system[38,39,40,41,42]. Assuming that the target photon direction is parallel to the beam axis, the polar angle θ^* of the μ^- and the azimuthal angle χ are defined as shown in Figure 10(b). Here χ is

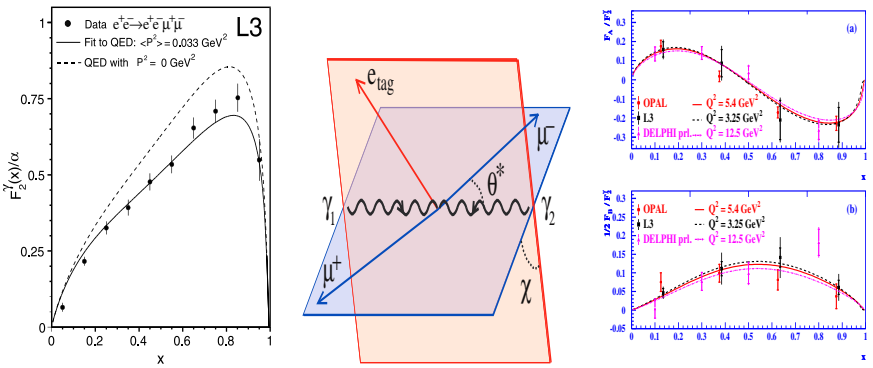

Figure 10. *(a) F_2^γ measured in the range $1.4 < \mathrm{Q}^2 < 7.6$ GeV^2, (b) definition of the angles θ^* and χ in the $\gamma\gamma$ centre of mass frame and (c) measurement of the F_A and F_B structure of function.*

the angle between the plane defined by the μ^- direction and the $\gamma\gamma$ axis, and the scattering plane of the tagged electron. Both structure functions F_A and F_B, originate from the interference terms of the scattering amplitudes. The characteristic x dependence of the interference terms, as predicted by QED, is observed in the data as shown in figure 10 (c). In particular F_A is due to the interference between longitudinal-transverse and transverse-transverse photon amplitudes, thus providing information on the longitudinal component of the probe photon. With this measurement, LEP proves that the longitudinal leptonic photon helicity amplitude can be accessed by the study of azimuthal correlations and is significantly non-zero.

7 Hadronic structure function $F_2^{\gamma,QCD}$

The measurement of the hadronic structure function, $F_2^{\gamma,QCD}$ has been performed at LEP in the range $0.0025 < x < 1$ and 1.2 GeV$^2 < Q^2 < 279$ GeV^2 [46,47,48,49]. The physical interest in the analysis of the hadronic photon structure function is twofold. Firstly, to measure the shape of F_2^γ, especially at small values of x, at fixed Q^2, where HERA experiments observe a strong rise of the proton structure function. Secondly the Q^2 evolution of F_2^γ is investigated. The F_2^γ measurements from L3 and OPAL are shown in Figure 11 (a) in the Q^2 interval from 1.2 to 9.0 GeV^2. The x range is $0.002 < x < 0.1$ at $\langle Q^2 \rangle = 1.9$ GeV^2 and $0.005 < x < 0.2$ at $\langle Q^2 \rangle = 5.0$ GeV^2. For the low val-

ues of x, the data agree better with the parton density prediction of GRV[43], whereas SaS-1d[45] prediction is lower.

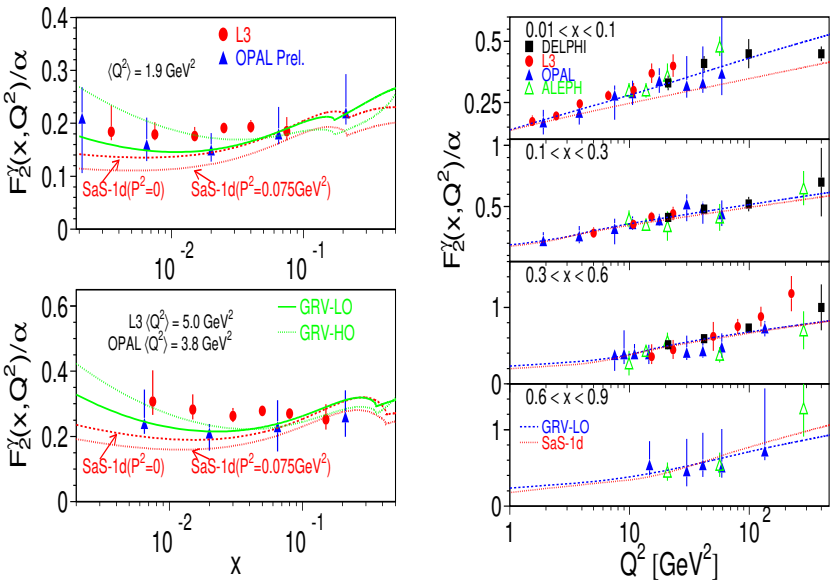

(a) (b)

Figure 11. *(a) The measured F_2^γ at $\langle Q^2 \rangle = 1.9$ GeV^2 and 5.0 GeV^2 and (b) evolution of F_2^γ as a function of Q^2 for different range of x values.*

A compilation of the results for different experiments on the Q^2 evolution of F_2^γ in various ranges of x are shown in Figure 11 (b). The measured values of F_2^γ show clearly the linear growth with $\ln Q^2$ expected by QCD. The predictions of the GRV-LO[43] and SaS-1d[45] models are also shown. With all the statistics available at the end of LEP data taking, one hopes to extract the effective scale parameter Λ_{QCD} at large x.

8 $\gamma^*\gamma^*$ Collisions

The cross-section of $\gamma^*\gamma^*$ collisions has been measured at LEP with L3[50] and OPAL[51] experiments in the range of 3 GeV^2 $< Q^2_{1,2} <$ 37 GeV^2. Since the two photons are highly virtual and unlike the proton, they do not contain constituent quarks with an unknown density distribution, so one may hope to have a complete perturbative QCD calculation under particular kinematical

conditions. An alternative QCD approach is based on the BFKL equation[52]. Here the highly virtual two-photon process, with $Q_1^2 \simeq Q_2^2$, is considered as the "golden" process where the calculation can be verified without phenomenological inputs[53,54]. The $\gamma^*\gamma^*$ interaction can be seen as the interaction of two $q\bar{q}$ pairs scattering off each other via multiple gluon exchange. In this scheme the cross-section for the collision of two virtual photons [53,54] depends upon the "hard Pomeron" intercept $\alpha_P - 1 = 0.53$[53,54] in the LO, whereas in the next-to-leading order the BFKL contribution is calculated to be smaller, $\alpha_P - 1 \simeq 0.17$[55]. The results from L3 and OPAL (figure 12(a)) show that the events are well described by the PHOJET Monte Carlo model which uses the GRV-LO parton density in the photon and leading order perturbative QCD. The LO BFKL calculations shown in the figure 12(b) with dotted line are too high. By leaving α_P as a free parameter in the LO calculations, a combined fit to the L3

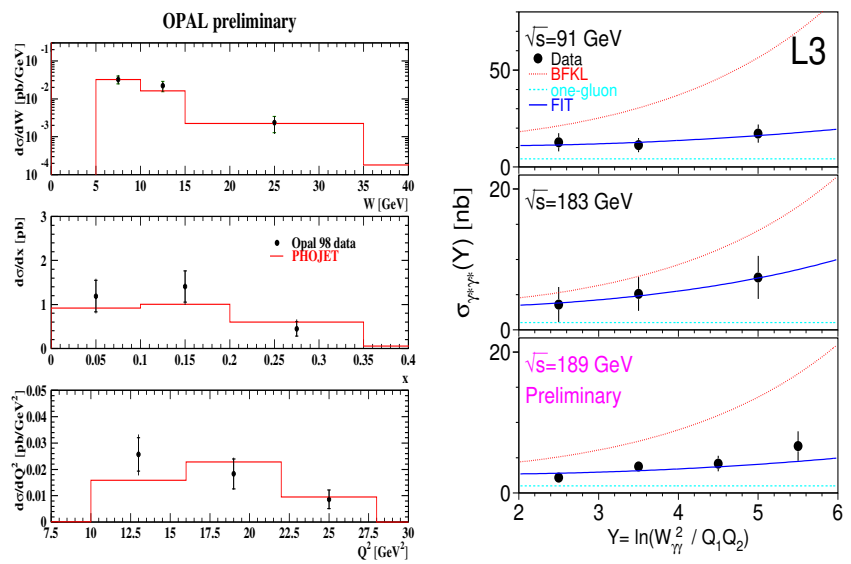

(a) (b)

Figure 12. *(a) The differential cross-section of double tag events compared to PHOJET Monte Carlo predictions and (b) the two photon cross-sections at LEP1 and LEP2 compared to LO-BFKL calculations after subtraction of the direct contribution*

data obtained at $\sqrt{s} \approx 91$, 183 and 189 GeV gives a value of $\alpha_P - 1 = 0.29 \pm 0.025$ with χ^2/d.o.f =7/9.

Outlook

Progress in the field of the two photon physics at LEP is significant, most notable are multi-hadron production and photon structure functions. With the statistics of 500 pb^{-1} luminosity available at the end of LEP II data taking, we expect not only large improvements in the understanding of the photon structure function at small x values but also have possibility to actually observe glueball states with very low two photon widths.

Acknowledgements

I would like to thank all the LEP colleagues for their contribution. I am grateful to J.H. Field and M.N. Kienzle-Focacci for encouraging discussions. This work is supported by the Swiss National Science Foundation.

References

1. L3 Coll., M. Acciarri et al., *Phys. Lett.* B **418**, 399 (1998)
2. L3 Coll., M. Acciarri et al., *Phys. Lett.* B **413**, 147 (1997)
3. L3 Coll., M. Acciarri et al., *Phys. Lett.* B **363**, 118 (1995)
4. L3 Coll., O. Adriani et al., Submitted to EPS, Tampere, 1999
5. L3 Coll., O. Adriani et al., *Phys. Lett.* B **286**, 403 (1992)
6. L3 Coll., O. Adriani et al., CERN-EP/99-072
7. OPAL Coll.,K. Ackerstaff et al., *Phys. Lett.* B **439**, 197 (1998);
   L3 Coll., M. Acciarri et al., *Phys. Lett.* B **453**, 73 (1999)
8. V.V. Anisovich et al., hep-ph/9702383
9. C. R. Münz, *Nucl. Phys.* A **609**, 364 (1996)
10. T. Feldmann and P. Kroll, *Phys. Lett.* B **413**, 410 (1997)
11. H. J. Lipkin, *Nucl. Phys.* B **7**, 321 (1968)
12. BES Coll., *Phys. Rev. Lett.* **76**, 3502 (1996)
13. Mark III Coll., *Phys. Rev. Lett.* **56**, 107 (1986)
14. B. Schrempp-Otto et al., *Phys. Lett.* B **36**, 463 (1971);
    G. Köpp et al., *Nucl. Phys.* B **70**, 461 (1974);
    P. Grassberger and R. Kögerler, *Nucl. Phys.* B **106**, 451 (1976)
15. P. D. B. Collins, Introduction to Regge theory (Cambridge U.P., Cambridge, 1977)
16. Review of Particle Physics, *Phys. Rev.* D **54**, 191 (1996)
17. L3 Coll., M. Acciarri et al., *Phys. Lett.* B **408**, 450 (1997);
    L3 Coll., M. Acciarri et al., Submitted to EPS, Tampere, 1999
18. OPAL Coll., G. Abbiendi et al., CERN-EP/99-076.

19. V. N. Gribov and L. Ya. Pomeranchuk, *Phys. Lett.* B **8**, 343 (1962).
20. A. Donnachie and P. V. Landshoff, *Phys. Lett.* B **296**, 227 (1992).
21. Review of Particle Physics, *Eur. Phys. J.* **C3** 205 (1998)
22. G. A. Schuler and T. Sjöstrand, *Nucl. Phys.* B **407**, 539 (1993);
    G. A. Schuler and T. Sjöstrand, *Z. Phys.* C **73**, 677 (1997)
23. R. Engel, *Z. Phys.* C **66**, 203 (1995);
    R. Engel and J. Ranft, *Phys. Rev.* D **54**, 4246 (1996)
24. R.M.Godbole and G.Pancheri, hep-ph/9903331 (1999)
25. OPAL Coll., K. Ackerstaff et al., *Eur. Phys. J* **C6**, 253 (1999)
26. J. Binnewies, B. A. Kniehl and G. Kramer, *Phys. Rev.* D **53**, 6110 (1996)
27. OMEGA Coll., R. J. Apsimon et al., *Z. Phys.* C **43**, 63 (1989)
28. OPAL Coll., K. Ackerstaff et al. , *Z. Phys.* C **73**, 433 (1997);
    OPAL Coll., G. Abbiendi et al. , *Eur. Phys. J* **C 6**, 253 (1999)
29. H. Kolanoski, Two-Photon Physics at e^+e^- Storage Rings, Springer-Verlag(1984);
    B. L. Combridge et al., *Phys. Lett.* B **70**, 234 (1977);
    D. W. Duke and J. F. Owens, *Phys. Rev.* D **26**, 1600 (1982)
30. M. Drees et al., *Phys. Lett.* B **306**, 371 (1993)
31. L3 Coll., M. Acciarri et al., Submitted to EPS, Tampere, 1999
32. OPAL Coll., G. Abbiendi et al. , Submitted to EPS, Tampere, 1999
33. ALEPH Coll., Contributed paper to Photon97 Egmond ann Zee, 1999.
34. DELPHI Coll., P. Abreu et al.,*Z. Phys.* C **96**, 199 (1994);
    DELPHI Coll., A. Zintchenko, PHOTON99, Freiburg, Germany
35. L3 Coll., M. Acciarri et al., *Phys. Lett.* B **436**, 403 (1998)
36. OPAL Coll., K. Ackerstaff et al., *Z. Phys.* C **60**, 593 (1993);
    OPAL Coll., K. Ackerstaff et al., *Z. Phys.* C **74**, 49 (1997);
    OPAL Coll., G. Abbiendi et al. , CERN-EP/99-010
37. V.M. Budnev et al., *Phys. Rep.* C **15**, 181 (1975)
38. CELLO Coll., H.J.Behrend et al., *Phys. Lett.* B **126**, 384 (1983)
39. P.Kessler, in Xth Int. Workshop on Gamma-Gamma Collisions, 1995, 281
40. Physics at LEP2, CERN96-01
41. C.Peterson,P.Zerwas and T.F.Walsh, *Nucl. Phys.* B **229**, 301 (1983)
42. R. Nisius and M. H. Seymour, *Phys. Lett.* B **452**, 409 (1999)
43. M. Glück, E. Reya and A. Vogt,*Phys. Rev.* D **45**, 3986 (1992);
    M. Glück, E. Reya and A. Vogt,*Phys. Rev.* D **46**, 1973 (1992)
44. H. Abramowicz, K. Charchula and A. Levy, *Phys. Lett.* B **269**, 458 (1991)
45. G. A. Schuler and T. Sjöstrand, *Z. Phys.* C **68**, 607 (1995);
    G. A. Schuler and T. Sjöstrand, *Phys. Lett.* B **376**, 193 (1996)

46. ALEPH Coll., R.Barate et al., *Phys. Lett.* B **458**, 152 (1999)
47. DELPHI Coll., Igor Tyapkin in " Workshop on Photon Interactions and the Photon structure", LUND 1998
48. L3 Coll., M. Acciarri et al., *Phys. Lett.* B **436**, 403 (1998);
    L3 Coll., M. Acciarri et al., *Phys. Lett.* B **447**, 147 (1999)
49. OPAL Coll., K. Ackerstaff et al., *Z. Phys.* C **74**, 33 (1997);
    OPAL Coll., K. Ackerstaff et al., *Phys. Lett.* B **411**, 387 (1997);
    OPAL Coll., K. Ackerstaff et al., *Phys. Lett.* B **412**, 225 (1997). OPAL Coll., G. Abbiendi et al., Submitted to EPS, Tampere, 1999
50. L3 Coll., M. Acciarri et al., *Phys. Lett.* B **453**, 333 (1999);
    L3 Coll., M. Acciarri et al., Submitted to EPS, Tampere, 1999
51. OPAL Coll., G. Abbiendi et al. , Submitted to EPS, Tampere, 1999
52. E.A. Kuraev, L.N. Lipatov and V.S. Fadin, Sov. Phys. JETP **45** (1977) 199;
    Ya.Ya. Balitski and L.N. Lipatov, Sov. J. Nucl. Phys. **28** (1978)822
53. S.J. Brodsky, F. Hautmann and D.E. Soper, *Phys. Rev.* D **56**, 6957 (1997)
54. J. Bartels, A. De Roeck and H. Lotter, *Phys. Lett.* B **389**, 742 (1996);
    J. Bartels, A. De Roeck, C. Ewerz and H. Lotter, hep-ph/9710500
55. S.J. Brodsky, V.S. Fadin, V.T. Kim, L.N. Lipatov and G.B. Pivovarov, hep-ph/99101229